SEISMIC RISK EVALUATION OF PLANT SITE USING EARTHQUAKE-TYPE DEPENDENT FRAGILITY CURVE

S. Fukushima[1], A. Satoda[2] , M. Oshima[3]

[1] *CEO, RKK Consulting Co., Ltd., fukushima@rkk-c.co.jp*
[2] *Senior Engineer, Chiyoda Corporation, satoda.akira@chiyodacorp.com*
[3] *Technical Expert, Chiyoda Corporation, oshima.masami@chiyodacorp.com*

Abstract

In the development of seismic fragility curve, Two kinds of approaches are generally employed; the one is empirical and the other is analysis-based. The empirical approach has been widely used since 1995 Kobe earthquake. The advantage of the method is that it can include various effects which are difficult to consider and to model. On the other hand, the disadvantage is that the results are data dependent so that the result may not be adequate in different situation. The advantage and disadvantage of the analysis-based approach are reverse of ones by empirical approach.

It is also noted that the difference in ground motion characteristics due to the difference in earthquake type is not considered in both approaches. Even though the ground motion intensity such as PGA or PGV is identical, the damage to the structure is earthquake dependent since spectral characteristics and time characteristics are different. One of approaches to solve the situation is to find the better ground motion parameters, and the other is to employ plural indices simultaneously using multi-event model.

As third approach, this paper propose to use earthquake-type dependent fragility. Concretely three kinds of earthquake type are employed, crustal earthquake, inter-plate earthquake and intra-plate earthquake. Though the multi-event model may conduct more precise evaluation, it is time consuming and is not adequate when risk at small exceedance probability is of concern. In other word, this approach considers the effect of spectral shape not in the seismic hazard analysis directly, but in the fragility analysis indirectly.

Seismic source zones downloaded from J-SHIS web site is used to generate numerous scenario earthquakes from the viewpoint of accountability. Response accelerations for some natural period corresponding to each model structures are used as ground motion parameters. For this, ground motion prediction equation by NIED is selected since it propose the attenuation for response acceleration.

As model plant site, selected is the Yokkaichi site prone to the large Nankai Trough earthquakes with high probability of occurrence. The model plant consists of several tanks with different diameter, several towers with different height and pipe racks. By providing various types of structures, it can be possible to examine the effects of earthquake types on seismic fragility curves.

Adequacy and effectiveness of earthquake-type dependent fragility is examined by the inclination of seismic risk curve.

Keywords: Seismic fragility, Earthquake type, Crustal earthquake, Inter-plate earthquake, Intra-plate earthquake

1. Introduction

In the development of seismic fragility curve, Two kinds of approaches are generally employed; the one is empirical and the other is analysis-based. The empirical approach has been widely used since 1995 Kobe earthquake. The advantage of the method is that it can include various effects which are difficult to consider and to model. On the other hand, the disadvantage is that the results are data dependent so that the result may not be adequate in different situation. The advantage and disadvantage of the analysis-based approach are reverse of ones by empirical approach.

It is also noted that the difference in ground motion characteristics due to the difference in earthquake type is not considered in both approaches. Even though the ground motion intensity such as PGA or PGV is identical, the damage to the structure is earthquake dependent since spectral characteristics and time characteristics are different. One of approaches to solve the situation is to find the better ground motion parameters, and the other is to employ plural indices simultaneously using multi-event model. For the former, a lot of researches have been conducted especially in the field of nuclear industry. The latter is a relatively new approch, which is proposed by Satoda *et al*.(2019) [1] also in the field of nuclear industry.

As third approach, this paper propose to use earthquake-type dependent fragility. Concretely three kinds of earthquake type are employed, crustal earthquake, inter-plate earthquake and intra-plate earthquake, since one of dominant factor that regulates the spectral shape is earthquake type and corresponding ground motion prediction equations are also proposed by many researchers.

2. Seismic Hazard Analysis at Plant Site

In order to conduct analysis-based fragility analysis, seismic hazard analysis at model site is conducted, followed by uniform hazard spectra corresponding to crustal, inter-plate and intra plate earthquakes.

2.1 Model site

Yokkaichi Industrial Complex in Mie prefecture is selected as model plant site as shown by J-SHIS Map [2] in Fig. 1, since the Yokkaichi city in Mie prefecture is located in the vicinity of many active faults and the Nankai Trough. It is noted that mega earthquakes have occurred on a 100 to 150 year recurrence period in the area along the Nankai Trough.

Source: J-SHIS Map

Fig. 1 Location of model site

2.2 Seismic source model and ground motion prediction equation

Seismic source model is constructed based on the database prepared by National Research Institute for Earth Science and Disaster Resilience (NIED) to assure the accountability. And ground motion prediction equation in NIED (2009) [3] is employed.

Figure 2 shows the uniform hazard spectra by all earthquakes, crustal earthquakes, inter-plate earthquakes and intra-plate earthquakes, respectively. Legend in each figure shows the return period. From the figure it can be seen that the uniform hazard spectrum by intra-plate earthquake is dominant when return period is short and the one by inter-plate earthquake is dominant when return period is long.

To examine the spectral shape, the uniform hazard spectra are normalized by the value at the shortest natural period as shown in Fig.3. It can be seen that the normalized uniform hazard spectra are almost identical regarding to return period except for one of 10 years, so the normalized uniform hazard spectra corresponding to return period of 1000 years are referred as target spectra for generation of input ground motion.

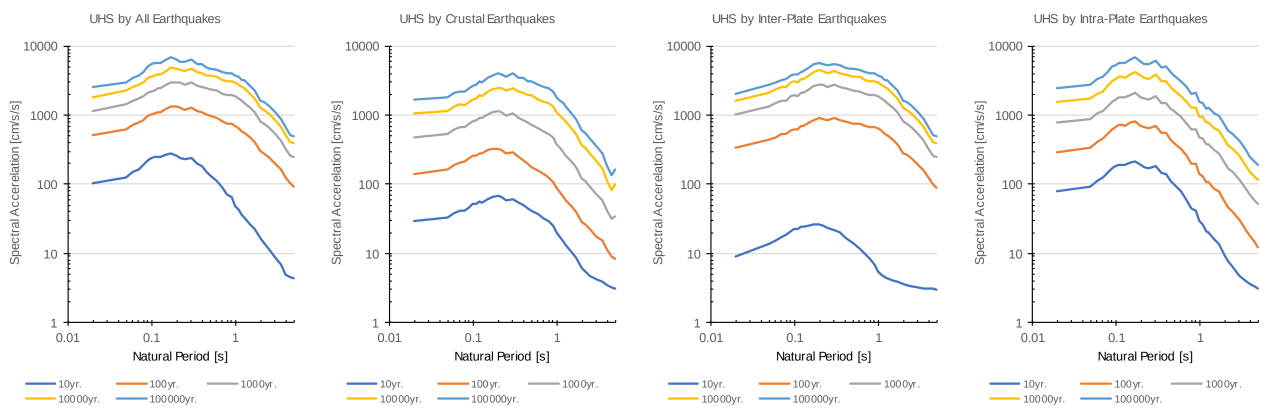

Fig. 2 Uniform hazard spectra at Yokkaichi site

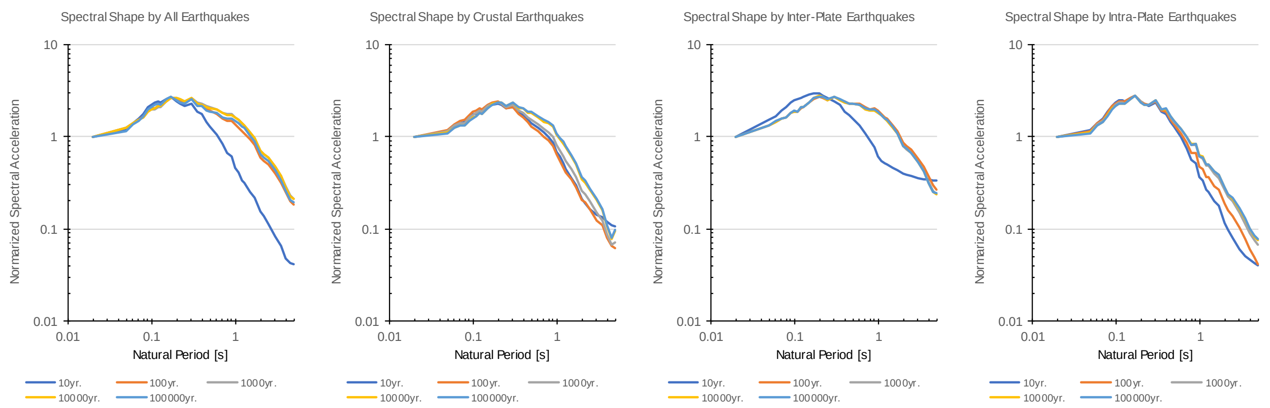

Fig. 3 Normalized uniform hazard spectra at Yokkaichi site

2.3 Generation of input ground motion for fragility analysis

For normalized UHS corresponding to annual exceedance probability of 0.001, 200 response spectra are generated assuming that the standard deviation about the median UHS is 0.2 in common logarithm. Also assumed is the inter-period correlation by Tanaka et al. (2008) [4], in which the correlation is given by Eq. (1),

$$\rho(t_1, t_2) = 1 - 0.308 \cdot abs\left[\ln\left(\frac{t_1}{t_2}\right)\right] \quad for\ t_1, t_2 \geq 0.1 \tag{1}$$

where, t_1 and t_2 are the periods of concern. In case t is smaller than 0.1, the correlation is assumed unity.

Figure 4 shows the 200 samples of response spectra of ground motions generated from normalized uniform hazard spectra. It is noted that the median of peak ground acceleration is normalized by 100 (cm/s/s). Fractiles of response spectra are also shown in Fig.5.

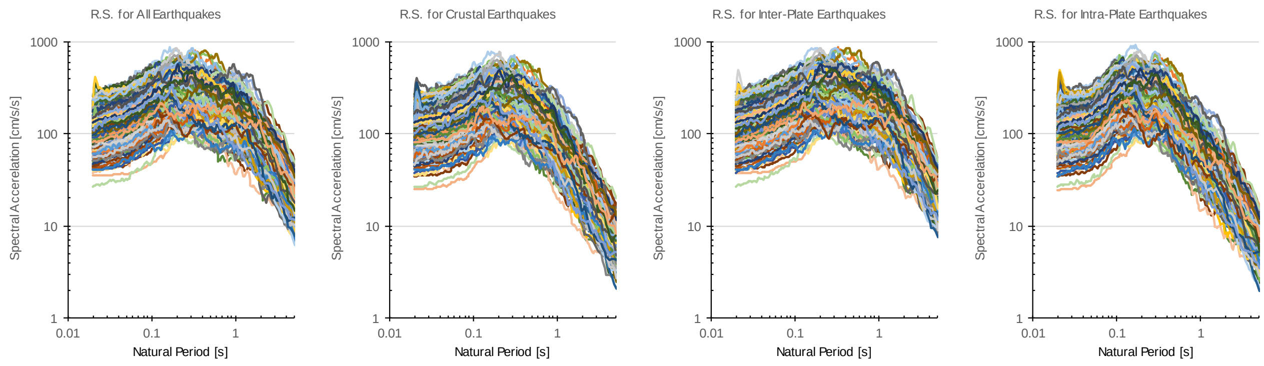

Fig. 4 Response spectra of input ground motion

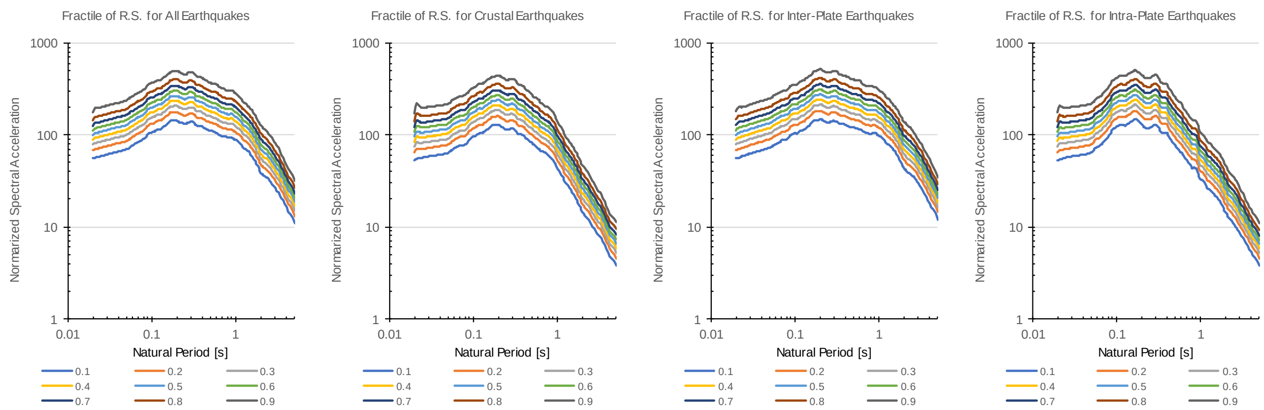

Fig. 5 Fractiles of response spectra of input ground motion

3. Seismic Fragility Analysis of Model Structure

Fragility curves of model structure is established analytically employing Monte-Carlo simulation.

3.1 Model structure

As model structure, selected are towers supported on skirt, whose specifications are summarized in Table 1. Towers are modelled as lumped mas model with fixed base, in which nodes are connected by linear beam elements. Specifications of models, such as mass, inertia, shear area and moment inertia are calculated using the data given in Table 1. Also given are Elastic modulus of material of 200,800 (N/mm2), Poisson's ratio of 0.3 and damping factor of 0.03.

Table 1 Specification of towers

Item	unit	Tower-1		Tower-2	
		Body	Skirt	Body	Skirt
High (Above the ground)	(mm)	10,000	1,220	30,000	3,660
Mean Diameter	(mm)	2,000	1,000	3,500	3,500
Thickness	(mm)	9	12	17	19
Operational Weight	(N/mm)	137.5	137.5	125.8	125.8

3.2 Result of simulation

The results of simulation is summarized in Fig. 6, in which median and natural logarithm standard deviation of bending moment are shown since flexure is dominant as mentioned in Satoda et al. (2017) [5]. The ground motion intensity is set to 100 (cm/s/s) for PGA.

Inter-plate earthquake and intra-plate earthquake are dominant for Tower-1 from the viewpoint of median, though the deference in response is not large. On the contrary, only inter plate-earthquake is dominant for Tower-2, since Tower-2 has longer natural period comparing to Tower-1 so that inter-plate earthquake excite the vibration of Tower-2.

There is small deference in standard deviations, among which that by inter-plate earthquake is the smallest.

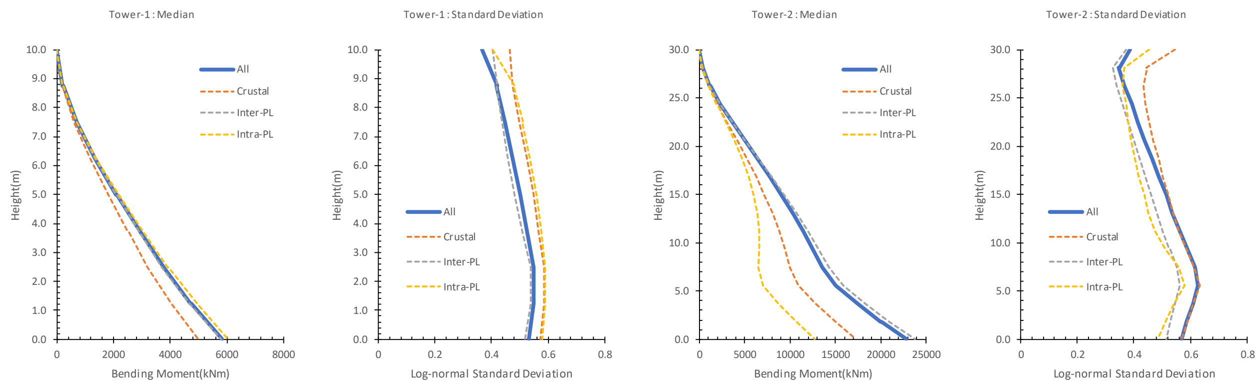

Fig. 6 Results of response analysis

3.3 Evaluation of seismic fragility curve

Seismic fragility of towers are assumed log-normally distributed, so that two parameters, median and log-normal standard deviation, are necessary to obtain seismic fragility curve. Seismic fragility curve $F(x)$ is given by Eq. (2),

$$F(x) = \Phi\left[\frac{\ln(x) - \ln(\bar{x})}{\zeta}\right] \tag{2}$$

where, $\Phi[\cdot]$ is normal distribution function, x is a ground motion intensity, $\bar{x}$ is a median capacity intensity, ζ is logarithmic standard deviation. It is noted that ζ is given in natural logarithm.

Authors assume that the failure of towers is dominated by flexural buckling, the median capacity intensity $\bar{x}$ is given by Eq. (3),

$$\bar{x} = \frac{\bar{M}}{m(x_R)} x_R = \frac{(\sigma_c - \sigma_0)Z}{m(x_R)} x_R \tag{3}$$

where, $\bar{M}$ is the median of buckling moment that is given by allowable buckling stress σ_c, permanent stress σ_c and section modulus Z. $m(x_R)$ is the median of resulting flexural moment for the input ground motion intensity x_R. Evaluation of σ_0 is based on the KHK(2012) [6]. Table 2 summarizes the parameters employed in Eq. (3).

Table 2 Summary of parameters used in Eq. (3)

Parameters	unit	Tower-1		Tower-2	
		Body	Skirt	Body	Skirt
Allowable buckling stress σ_c	(N/mm^2)	165.00	199.0	165.00	199.0
Permanent stress σ_0	(N/mm2)	25.11	17.02	21.80	17.40
Section modulus Z	(m^3)	0.028	0.037	0.162	0.181
Median of buckling moment $\bar{M}$	(kN m)	3,920	6,779	23,197	32,841

Authors also assume that the buckling occurs in the tower at the top of skirt or in the skirt at the base. Using the Eq. (3), the median capacity intensity $\bar{x}$ is calculated for each ground motion intensity. The natural log-normal deviation is given by response analysis as shown in Fig. 6. Other variability factors for capacity intensity, such as the variabilities in material strength and damping, are ignored, since they are negligible. Table 3 summarizes the acceleration capacity.

Table 3 Summary of acceleration capacity

Earthquake	Parameters in Eq. (6)	unit	Tower-1		Tower-2	
			Body	Skirt	Body	Skirt
All Earthquake	x_R	(cm/s/s)	100	100	100	100
	$m(x_R)$	(kN m)	4,729	5,818	17,427	22,801
	$\bar{x}$	(cm/s/s)	82.9	116.5	133.1	144.0
	ζ	-	0.548	0.531	0.610	0.568
Crustal Earthquake	x_R	(cm/s/s)	100	100	100	100
	$m(x_R)$	(kN m)	4,026	4,969	12,876	17,262
	$\bar{x}$	(cm/s/s)	97.4	136.4	180.2	190.2
	ζ	-	0.587	0.574	0.610	0.570
Inter-Plate Earthquake	x_R	(cm/s/s)	100	100	100	100
	$m(x_R)$	(kN m)	4,679	5,788	18,340	23,802
	$\bar{x}$	(cm/s/s)	83.8	117.1	126.5	138.0
	ζ	-	0.538	0.517	0.547	0.514
Intra-Plate Earthquake	x_R	(cm/s/s)	100	100	100	100
	$m(x_R)$	(kN m)	4932	6039	8721	12756
	$\bar{x}$	(cm/s/s)	79.5	112.3	266.0	257.5
	ζ	-	0.588	0.578	0.543	0.486

Figure 7 shows the seismic fragility curves using values in Table 3. It may be concluded that the fragility of tower is dominated by that of body rather than by skirt, though the fragility is almost identical in case of Tower-2 for intra-plate earthquake. Therefore, fragility of body will be focused hereafter.

Figure 8 compares the fragility curves by earthquake type regarding to body as described above. Failure probability of Tower-1 will be overestimated for crustal earthquake and that of Tower-2 will be done so for crustal and intra-plate earthquakes comparing to using fragility curve derived from all earthquakes. On the contrary, failure probability of Tower-2 will be somewhat underestimated for inter-plate earthquake.

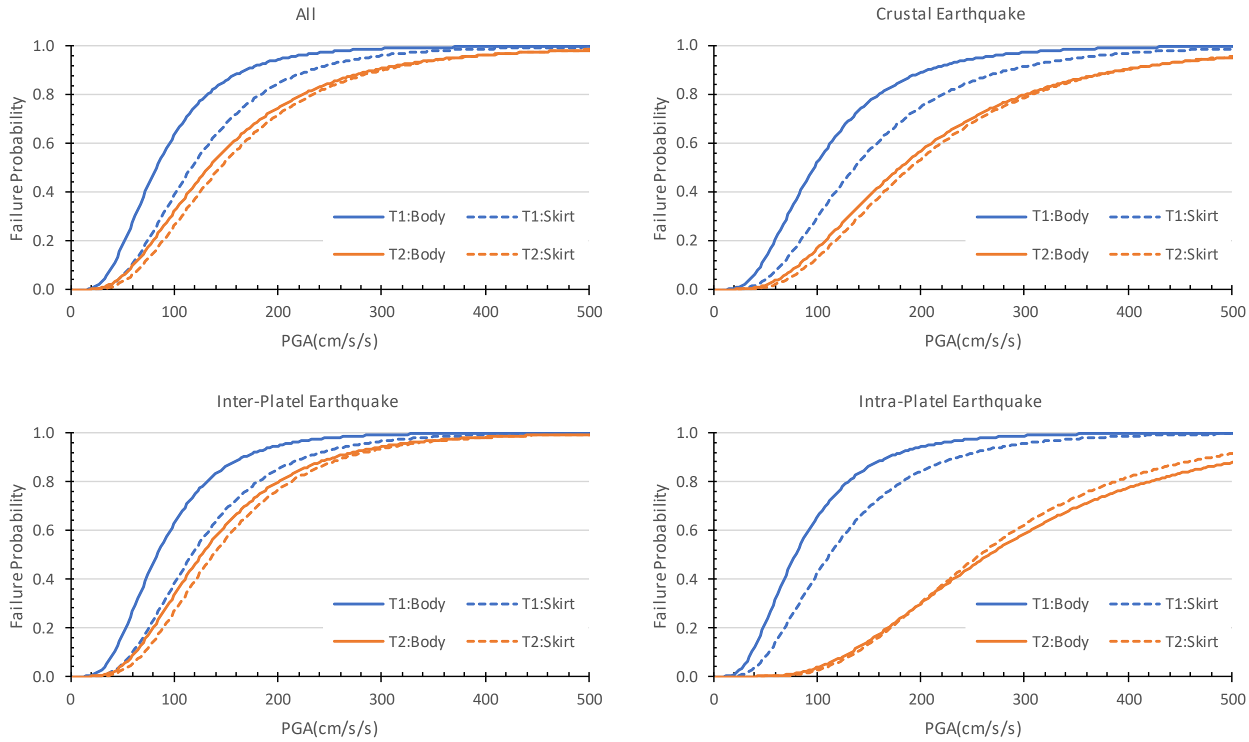

Fig. 7 Comparison of fragility curves by structure

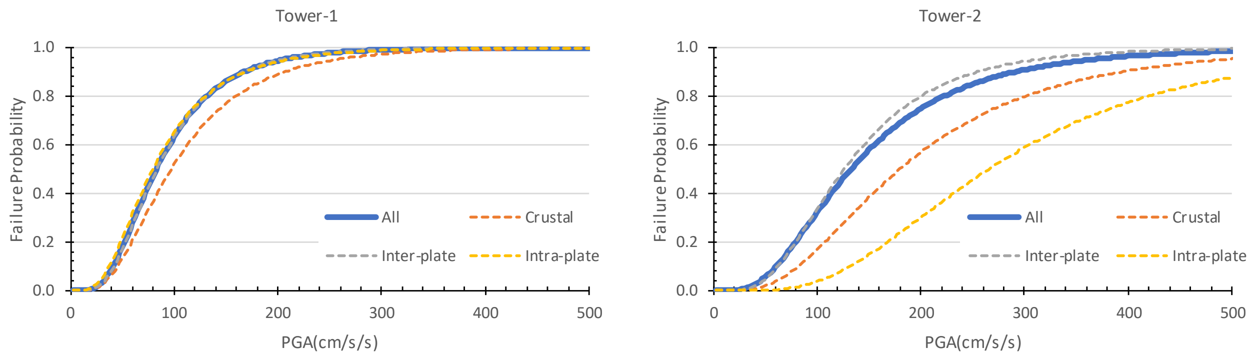

Fig. 8 Comparison of fragility curves by earthquake-type

4. Risk Analysis

In order to conduct risk analysis using earthquake-type dependent fragility curves, employed is the multi-event model by which risk of concern will be evaluated for numerous discretized earthquakes with their location, magnitude, shape, annual occurrence frequency.

4.1 Outline of multi-event model

Authors employ the multi-event model which evaluates the probability of risk value for each event with annual occurrence probability and integrates them to produce risk curve. Figure 9 shows the flowchart of risk analysis based on multi-event model.

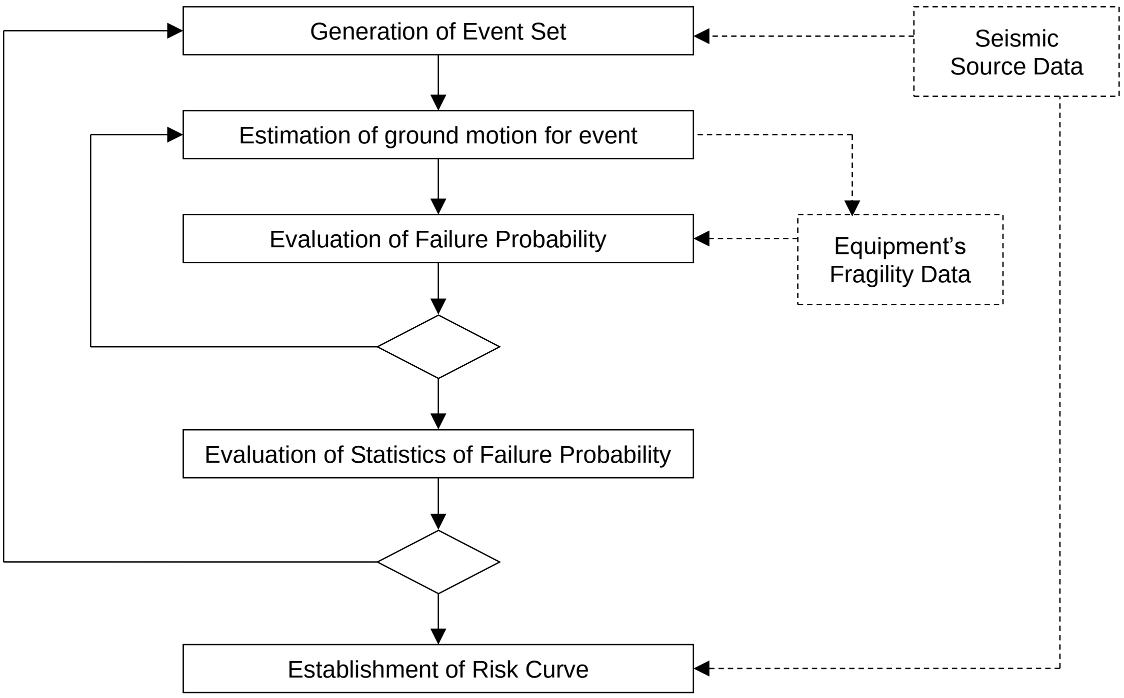

Fig. 9 Flowchart of risk analysis based on multi-event model

At first, event set is generated from seismic source data. Then events that will give damage to equipment is selected considering seismic magnitude and distance from site, followed by estimation of ground motion intensity using attenuation relation. It is noted that the source data and attenuation relation same as the ones used in evaluation of uniform hazard spectra were employed in this application.

For the ground motion intensity by each event, failure probability is calculated using the fragility curve corresponding to the event. It is noted that failure probability is employed as risk value in this application.

Above step is repeated as Monte-Carlo simulation, so that statistics of failure probability is obtained. And the Monte-Carlo simulation is conducted for each event to establish risk curve.

4.2 Establishment of risk curve

Let R_i be the risk value for event i. So annual exceedance probability of the risk value $y_{j,i}$ for event i is given by the following equation,

$$y_{j,i} = \nu_i \cdot P(R_i > x_j) \quad (4)$$

where, ν_i is annual occurrence frequency of event i, x_j is j th threshold.

Since events are independent to one another, annual exceedance probability of the risk value Y_j is given as follows,

$$Y_j = \sum_{i=1}^{n} y_{j,i} \quad (5)$$

where, n is the number of events. By repeating this step for every thresholds, risk curve that is the relationship between threshold and annual exceedance probability of risk value is obtained.

4.3 Results

Figure 10 shows the risk curves for Tower-1 and Tower-2 derived by the proposed method. It can be seen that intra-plate earthquake is dominant for both equipment. For Tower-1, deference in contribution of inter-plate earthquake and intra-plate earthquake appears though fragility curves by inter-plate earthquake and one by intra-plate earthquake are almost identical. This is due to low occurrence probability of inter-plate earthquake.

For Tower-2, contribution of inter plate earthquake is small in the range of low failure probability though fragility by the earthquake is the biggest as shown in Fig.8. This is also due to its low occurrence probability. On the other hand, inter-pate earthquake becomes dominant in the range of high failure probability.

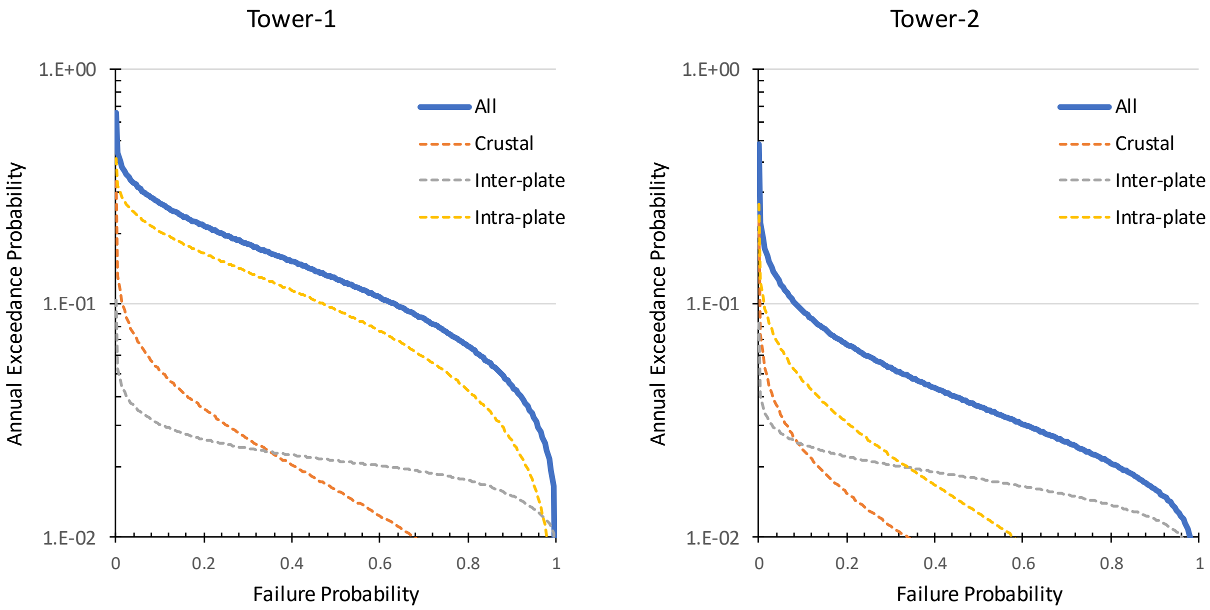

Fig. 10 Risk curves by proposes method

Figure 11 shows the comparison of risk curve by proposed method and on by previous method. It is noted that the previous method means the analysis-based method using earthquake-type independent fragility.

For Tower-1 both methods give almost same risk curve, since the fragility curve of intra-plate earthquake that is the dominant earthquake is identical with one for all earthquakes. Let spectral ratio be the ratio of spectral acceleration at given natural period to PGA here. Spectral ratio of Tower-1 whose natural period is 0.3s remains same by earthquake type, so that the deference in earthquake type does not appear in risk curve as well as seismic fragility curve.

The large difference in risk curve can be observed in Tower-2, since the fragility of dominant intra-plate earthquake is considerably small as shown in Fig.8. This is due to the spectral ratio of Tower-2 whose natural period is 0.8s.

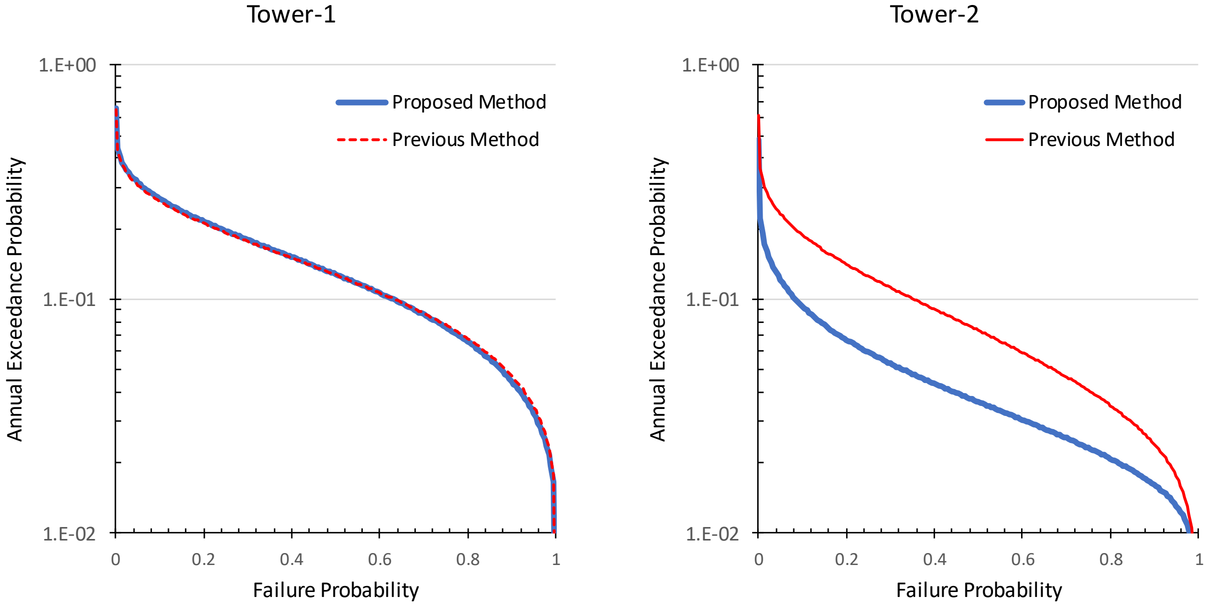

Fig. 11 Comparison of risk curves

5. Conclusions

Authors have conducted probabilistic risk evaluation of petrochemical plant structures using PGA as ground motion intensity. However plant sites consist of various structures and equipment with various natural period, for which PGA is not a good risk estimator since it does not contain the information on spectral shape. So far two approaches are conducted to solve the issue, one is to establish better estimator, and the other is to use plural estimator simultaneously.

This paper proposed the third approach, by which the effect of spectral shape is introduced not in seismic hazard but in seismic fragility. To make this approach conductive, the multi-event model was introduced.

The effectiveness of the method was examined by model plant site consisting of two towers whose natural periods are 0.3s and 0.8s, respectively. At first, some sets of ground motions were developed based on the UHS at Yokkaichi site, followed by normalization by PGA. Then seismic fragility curves of towers were developed by Monte-Carlo simulation using each set of ground motion. The fragility curves identified critical failure mode of towers, which was the buckling of the body by flexure.

Comparison of fragility curve regarding to earthquake type showed that fragility curves are deferent if the earthquake-type of concern is different. So it can be concluded that it is rational and adequate to use fragility curves corresponding to earthquake type. This conclusion was also proved by comparing risk curves. In application it was demonstrated that risk gets smaller if the fragility of dominant earthquake is smaller. Of course, the result can be opposite if the fragility of dominant earthquake is larger.

In future, more precise categorization of event, such as by magnitude or by focal depth, will be examined to conduct more realistic risk evaluation. Especially the deference in duration time that affect nonlinear behavior of structure can be considered in fragility analysis, if seismic magnitude is employed in categorization of event.

6. References

[1] Satoda A, Fukushima S, Oshima M (2019): Evaluation of plant risk based on multi-event model. *Transactions SMiRT 25*, Charlotte, USA.

[2] NIED (National Research Institute for Earth Science and Disaster Prevention): Japan Seismic Hazard Information Station, http://www.j-shis.bosai.go.jp/en/, Japan.

[3] NIED (National Research Institute for Earth Science and Disaster Prevention) (2009): A Study on National Seismic Hazard Maps for Japan, *Technical Note of NIED No.336*, Japan. (in Japanese)

[4] Tanaka, K., Wang, M., Takada, T. (2008): Covariance structure between spectral accelerations with different periods and its application, *J. Struct. Const. Eng.*, AIJ, Vol.73, No.632, 1727-1733. (in Japanese)

[5] Satoda, A., Oshima, M. (2017): Method for the evaluation of seismic risk and cost-effective strengthening of plant facilities, *Transaction of 24th SMiRT*, Busan, South Korea.

[6] KHK (2012): Seismic Design Code of High Pressure Gas Facilities, The High Pressure Gas Safety Institute of Japan

